Environmental Pollution 182 (2013) 80–91

Contents lists available at SciVerse ScienceDirect

Environmental Pollution

journal homepage: www.elsevier.com/locate/envpol

A multi-isotope approach for estimating industrial contributions to atmospheric nitrogen deposition in the Athabasca oil sands region in Alberta, Canada

Bernadette C. Proemse [a,*], Bernhard Mayer [a], Mark E. Fenn [b], Christopher S. Ross [b]

[a] Department of Geoscience, University of Calgary, 2500 University Drive NW, Calgary, Alberta T2N 1N4, Canada
[b] USDA Forest Service, Pacific Southwest Research Station, 4955 Canyon Crest Drive, Riverside, CA 92507, USA

ARTICLE INFO

Article history:
Received 18 December 2012
Received in revised form
24 May 2013
Accepted 5 July 2013

Keywords:
Atmospheric nitrate
Nitrogen isotopes
Oxygen isotopes
Deposition
Throughfall
Oil sands
Oxygen-17
Athabasca
Alberta

ABSTRACT

Industrial nitrogen (N) emissions in the Athabasca oil sands region (AOSR), Alberta, Canada, affect nitrate (NO_3) and ammonium (NH_4) deposition rates in close vicinity of industrial emitters. NO_3–N and NH_4–N open field and throughfall deposition rates were determined at various sites between 3 km and 113 km distance to the main oil sand operations between May 2008 and May 2009. NO_3 and NH_4 were analyzed for $\delta^{15}N–NO_3$, $\delta^{18}O–NO_3$, $\Delta^{17}O–NO_3$ and $\delta^{15}N–NH_4$. Marked differences in the $\delta^{18}O$ and $\Delta^{17}O$ values between industrial emissions and background deposition allowed for the estimation of minimum industrial contributions to atmospheric NO_3 deposition. $\delta^{15}N–NH_4$ values also allowed for estimates of industrial contributions to atmospheric NH_4 deposition. Results revealed that particularly sites within ~30 km radius from the main oil sands developments are significantly affected by industrial contributions to atmospheric NO_3 and NH_4 deposition.

© 2013 Elsevier Ltd. All rights reserved.

1. Introduction

The Athabasca oil sands in northeastern Alberta, Canada, constitute an enormous heavy oil resource that is becoming increasingly important for the Canadian economy as the availability of conventional fossil fuel reserves continues to decline. This unconventional oil resource has experienced an unprecedented expansion of mining projects (open pit mining) and in-situ operations (e.g. steam-assisted gravity drainage) over the last decade. The bitumen is extracted from the mined oil sand and upgraded to synthetic crude oil while removing excess nitrogen and sulfur. Both mining and upgrading of bitumen are accompanied by significant industrial nitrogen (N) emissions, including stack emissions, vehicle emissions from heavy haulers operating in the open pit mines and other off- and on-road vehicles, among others. NO_x (nitrogen oxides) emissions have increased by 29% in Western Canada between 1985 and 2000 contrasting with declines observed in Eastern Canada (Schindler et al, 2006). The potential consequences of elevated N emissions are diverse, including acid deposition and eutrophication of terrestrial and aquatic ecosystems (Galloway et al., 2008; Gruber and Galloway, 2008). Acid deposition, soil acidification and the potential of N saturation are particularly of concern in the typically N-limited boreal forest ecosystems of the Athabasca oil sands region (AOSR) (Laxton et al., 2012; Jung and Chang, 2012; Jung et al., 2011; Cheng et al., 2011; Ok et al., 2007; Whitfield et al., 2009; Wieder et al., 2010). Hence, monitoring of atmospheric N deposition and a better understanding of nitrogen transport from industrial sources to sinks in terrestrial and aquatic ecosystems are crucial for a thorough assessment of environmental effects of elevated nitrogen emissions and deposition in the AOSR.

Nitrogen isotope ratios have been successfully used in some case studies of the atmospheric N cycle determining the sources and fate of anthropogenic atmospheric nitrogen (e.g. Elliott et al., 2007; Nanus et al., 2008). However, the usefulness of nitrogen isotope ratios to trace N emissions is often limited due to significant variability observed for $\delta^{15}N$ values of atmospheric nitrate (NO_3) and ammonium (NH_4) (Freyer, 1991; Garten, 1992; Hastings et al., 2004), wide ranges of nitrogen isotope ratios observed for potential NO_x sources, and possible isotope fractionation during nitrogen conversion reactions (Moore, 1977; Ammann et al., 1999; Pearson

* Corresponding author.
E-mail address: bcpromse@ucalgary.ca (B.C. Proemse).

0269-7491/$ – see front matter © 2013 Elsevier Ltd. All rights reserved.
http://dx.doi.org/10.1016/j.envpol.2013.07.004

et al., 2000). As a consequence, $\delta^{15}N$ values of atmospheric nitrate and ammonium can vary from $<-15‰$ to $>+15‰$ (Kendall et al., 2007). It is also possible to determine the oxygen isotope ratios ($^{18}O/^{16}O$, $^{17}O/^{16}O$) of atmospheric nitrate, which have been shown to be enriched in both ^{18}O and ^{17}O due to reactions involving ozone (O_3) that is anomalously enriched in the heavy oxygen isotopes (Durka et al., 1994; Kendall et al., 2007; Michalski et al., 2003). Oxygen-17 contents are typically expressed as $\Delta^{17}O$ ($\Delta^{17}O = \delta^{17}O - 0.52*\delta^{18}O$) in per mil (‰). Recently, $\Delta^{17}O$ of stack emitted nitrate in $PM_{2.5}$ from one of the oil sands facilities has been reported to be near 0‰ (Proemse et al., 2012a) and therefore this nitrate is distinct from atmospheric nitrate with $\Delta^{17}O$ values that typically range between 20 and ~31‰ (Michalski et al., 2003), providing a potential tracer for industrial nitrate emissions. $\delta^{18}O$ values of nitrate in $PM_{2.5}$ emitted from industrial point sources have also been shown to have low values (~18‰) (Proemse et al., 2012a) compared to $\delta^{18}O$ values of atmospheric nitrate (~60–~95‰) (Kendall et al., 2007). Hence $\delta^{18}O$ and $\Delta^{17}O$ values of nitrate in atmospheric deposition are not only capable of revealing oxidation pathways of nitrogen compounds in the atmosphere (Michalski et al., 2003; Morin et al., 2008; Savarino et al., 2007), but may possibly also fingerprint sources of nitrate. However, no studies of the isotopic composition of nitrogen compounds in atmospheric deposition have been reported for Western Canada or the Athabasca oil sands region in particular. To fill this knowledge gap, atmospheric nitrate and ammonium were collected in open field and throughfall deposition samplers located at various distances from industrial emission sources in the AOSR for two years (2007–2009). The objectives of this study were: 1) to test whether stable isotope techniques ($\delta^{18}O$, $\Delta^{17}O$, $\delta^{15}N$) have the potential to trace industrial contributions to atmospheric nitrogen deposition in the vicinity of industrial emitters in the AOSR, and if so, 2) to quantify N contributions from industrial emission sources to NO_3 and NH_4 deposition in the Athabasca oil sands region.

2. Materials and methods

2.1. Study area

The Athabasca oil sands region is the largest of three oil sand reservoirs in Alberta, Canada (Peace River, Cold Lake, Athabasca). These oil sands operations are surrounded by a mixture of peatlands and upland forest ecosystems including jack pine, spruce and aspen. The upland forests often grow on an eluviated Dystric Brunisol consisting mostly of sand (Soil Classification Working Group, 1998). Annual precipitation in Fort McMurray (Fig. 1) is 455.5 mm and the mean annual temperature is 0.7 °C (30-year-average (1971–2000), Environment Canada, 2011). Precipitation rates are typically highest during the summer months. The prevailing wind direction is from the West and Northwest (Sandhu and Blower, 1986), but varies with season (Government of Alberta, 2011) and terrain (Leahey and Hansen, 1982).

Sixteen sampling sites established by the Terrestrial Environmental Effects Monitoring (TEEM) group of the Wood Buffalo Environmental Association (WBEA) were selected based on numerous site selection criteria (AMEC, 2001) for collection of open field bulk deposition (wet deposition + dry deposition) and throughfall deposition (bulk deposition underneath tree canopy) between April 2007 and May 2009. In areas where dry deposition constitutes a major component of atmospheric deposition, throughfall deposition rates are a better indicator of atmospheric N input and availability in an ecosystem because it contains dry deposition scavenged by the tree canopy. A major emission stack from one of the oil sands operators near Fort McMurray (57.0479875 °N, 111.615502 °W) was used as a central marker point and distances from marker to sampling sites vary between 3 and 113 km. However, this site is not the only source of industrial N emissions as there are several other oil sand processing plants and open pit mines in the AOSR that are associated with stack and vehicle emissions (e.g. from heavy haulers among others). The expanding town of Fort McMurray and the frequent forest fires in northeastern Alberta (Larsen, 1997) represent other potential sources of atmospheric N in the region.

Four of the sampling sites have existed since April 2007 (JP102, JP212, JP213 and JP107), and twelve additional sites were established in May 2008 (AMS 1, AMS 5, AMS 9, AMS 10, AMS 13, AMS 14, AMS 15, LYS, JP104, W1, Peat Pond, R2) (Fig. 1). The sites AMS 5, AMS 9, AMS 10, AMS 15, LYS, W1 and Peat Pond are located on land leased by industry and will therefore be referred to as industrial sites. AMS 1 (Fort MacKay) and AMS 14 (Anzac) are located in small communities. AMS 14 is also close to an in-situ operation including a bitumen upgrader. The sites JP104, JP102, JP212, JP213, JP107 and R2 are forest health plots at upland forest sites.

2.2. Sample collection and concentration analyses

Nitrate (NO_3^-) and ammonium (NH_4^+) in bulk deposition were sampled using an ion exchange resin (PVC tubes containing ion exchange resin beads) method (Fenn and Poth, 2004; Fenn et al., 2009). At each of the 16 sites, four open field (bulk deposition) samplers were installed in clearings in the boreal forest. In addition, eight throughfall samplers were mounted on jack pine trees (Fenn and Ross, 2010). Resins were typically exposed for approximately half-year periods. The results from the following 4 sampling periods are presented: April 2007 to September 2007 ("summer 2007") and October 2007 to May 2008 ("winter 2007/2008") for four different sites (JP107, JP102, JP212, JP213), and May 2008 to October 2008 ("summer 2008") and October 2008 to May 2009 ("winter 2008/2009") for all 16 sites.

In the laboratory, the ion exchange resins were quantitatively eluted with 1N KI (Simkin et al., 2004). Nitrate concentrations in the KI extracts were analyzed using ion chromatography and NH_4 concentrations were determined colorimetrically, and deposition rates for the exposure periods were determined at the USDA Forest Service Laboratory, Riverside (California, USA). Annual deposition rates for the year May 2008 to May 2009 were calculated by adding summer 2008 deposition rates to winter 2008/2009 deposition rates. Sub-samples of the eluted solutions were subsequently shipped to the University of Calgary (Alberta, Canada) for isotopic analyses of nitrate ($\delta^{15}N–NO_3$ and $\delta^{18}O–NO_3$, $n = 455$) and ammonium ($\delta^{15}N–NH_4$, $n = 134$). $\Delta^{17}O$ of nitrate was analyzed on 30 sub-samples at the University of Washington in Seattle (WA, USA).

2.3. Isotope analyses

Nitrogen isotope ratios ($\delta^{15}N$) and oxygen isotope ratios ($\delta^{18}O$) of nitrate were analyzed by isotope ratio mass spectrometry (IRMS) using N_2O gas generated via the bacterial denitrification method (Sigman et al., 2001; Casciotti et al., 2002). Results are reported in the internationally accepted δ notation defined as

$$\delta_{\text{sample}}(‰) = \left[\left(R_{\text{sample}}/R_{\text{standard}}\right) - 1\right]*1000 \quad (1)$$

where R is the $^{15}N/^{14}N$ or $^{18}O/^{16}O$ ratio of the sample and a standard respectively. $\delta^{15}N$ values are reported relative to AIR and $\delta^{18}O$ relative to Vienna Standard Mean Ocean Water (VSMOW). The international reference materials IAEA KNO_3 and USGS 34, and in-house laboratory standards were used to ensure accuracy and long-term external precisions of ±0.5‰ and ±1.0‰ for $\delta^{15}N$ and $\delta^{18}O$ values of nitrate, respectively.

$\Delta^{17}O–NO_3$ values were determined using a modified bacterial denitrification method (Kaiser et al., 2007). $\Delta^{17}O–NO_3$ is reported as the deviation of $\delta^{17}O$ from the mass dependent relationship ($\delta^{17}O = 0.52*\delta^{18}O$) and expressed as $\Delta^{17}O$ ($\Delta^{17}O = \delta^{17}O - 0.52*\delta^{18}O$). Each sample was analyzed in duplicate. The long-term external precision based on measurements of USGS 32, USGS 34, USGS 35, IAEA KNO_3 and sample replicates was 0.6‰.

$\delta^{15}N$ of ammonium (NH_4^+) was measured using the ammonium diffusion method (Sebilo et al., 2004). The international reference material IAEA-N-2, an in-house standard, and a blank were included in each sample set to assure accuracy. $\delta^{15}N–NH_4$ values were determined using an elemental analyzer interfaced with an isotope ratio mass spectrometer (IRMS). Accuracy and precisions of $\delta^{15}N$ values of ammonium samples were ensured using the reference materials USGS 40 and USGS 41 and the external precision of $\delta^{15}N–NH_4$ values using the ammonium diffusion method was ±0.6‰.

For each collection period, N-deposition weighted mean values for samples from several collectors at one site were calculated for $\delta^{15}N–NH_4$, $\delta^{15}N–NO_3$ and $\delta^{18}O–NO_3$ in open field deposition and throughfall, but it was not possible to calculate averages for $\Delta^{17}O$ values due to the low number of measurements ($n = 30$). Both N-deposition weighted site averages and the non-deposition weighted individual measurements are reported here. Average $\delta^{15}N$ and $\delta^{18}O$ values of atmospheric nitrate and ammonium from open field deposition and throughfall samplers were determined by calculating deposition-weighted means ($\bar{x}$) per site and sampling period according to

$$\bar{x} = \frac{\sum_{i=1}^{n} w_i x_i}{\sum_{i=1}^{n} w_i} \quad (2)$$

where w_i is the deposition rate and x_i the isotope ratio of the sample i.

3. Results

3.1. Ammonium deposition rates

Yearly ammonium ($NH_4–N$) deposition rates for the sixteen sampling sites monitored between May 2008 and May 2009 varied

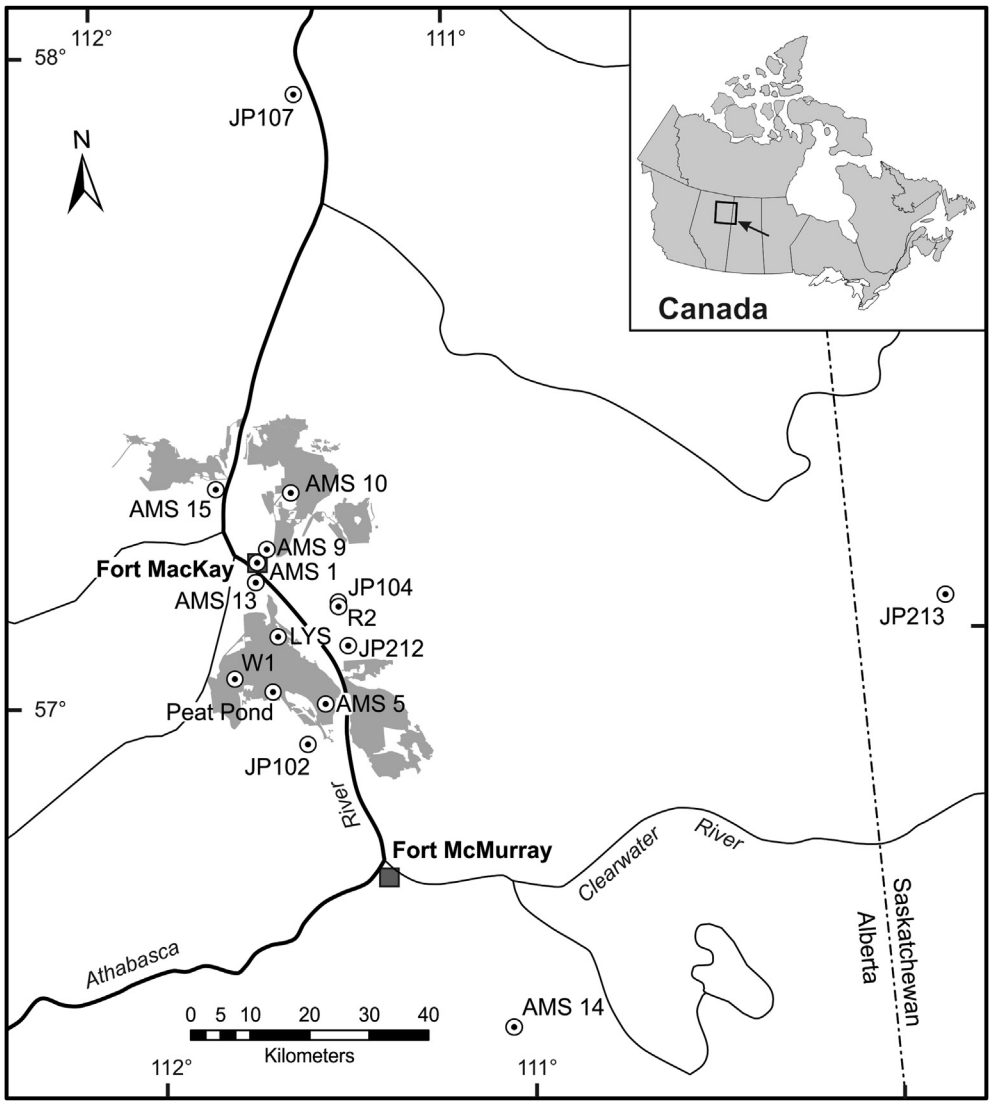

Fig. 1. The Athabasca oil sands region in northeastern Alberta, Canada, showing the sampling site locations for ammonium and nitrate deposition collectors (circles), towns (black boxes), and the open pit mining sites as of 2008 (gray shaded areas).

between 1.0 kg N ha^{-1} yr^{-1} and 4.7 kg N ha^{-1} yr^{-1} for open field deposition and between 1.0 kg N ha^{-1} yr^{-1} and 18.3 kg N ha^{-1} yr^{-1} for throughfall. On average, yearly ammonium deposition rates in throughfall were twice as high as those in open field deposition, but there was no difference in open field deposition and throughfall deposition rates at the forest health plots 94 and 113 km distant from the emission sources (JP107 and JP213, Fig. 2a). The highest deposition rate (18.3 kg N ha^{-1} yr^{-1}) was observed in throughfall at the LYS site, 3 km away from the emission stack. Annual NH_4–N deposition rates were dominated by the summer 2008 deposition inputs due to high precipitation rates during summer 2008 (Fig. 2a).

3.2. Nitrate deposition rates

Annual nitrate deposition rates (NO_3–N) for the sixteen sampling sites monitored from May 2008 to May 2009 varied between 0.5 and 2.0 kg N ha^{-1} yr^{-1} for open field deposition samples, and between 0.3 and 11.0 kg N ha^{-1} yr^{-1} for throughfall samples. NO_3–N deposition rates were lowest (<0.5 kg N ha^{-1} yr^{-1}) for forest health plots most distant (>90 km) from the industrial emission sources and highest for both open field deposition (2.0 kg N ha^{-1} yr^{-1}) and throughfall (11.0 kg N ha^{-1} yr^{-1}) at the industrial site AMS 5, 12 km east of the emission stack (Fig. 2b). On average, throughfall deposition rates were about twice as high as the open field deposition rates. However, throughfall samples from forest health plots >90 km from the emission stack had yearly NO_3–N deposition rates as low as 0.3 kg N ha^{-1} yr^{-1}, slightly lower than those of the co-located open field samplers (~0.5 kg N ha^{-1} yr^{-1}). Annual nitrate deposition fluxes were also dominated by summer 2008 deposition rates (Fig. 2b).

3.3. $\delta^{15}N$ of ammonium in atmospheric deposition

The NH_4–N-deposition-weighted, site-averaged nitrogen isotope ratios of ammonium in open field and throughfall samples varied between −6.3 and +11.3‰ (Fig. 3a). $\delta^{15}N$–NH_4 values at sites at 74, 94 and 113 km distance were less variable ranging from −4.1 to +3.3‰, with an average of −0.9‰. Nitrogen isotope ratios of ammonium were more variable closer (<29 km) to the emission sources (−6.3 to +11.3‰). $\delta^{15}N$–NH_4 values >+4‰ were only observed within 18 km distance of the emission stack (Fig. 3a).

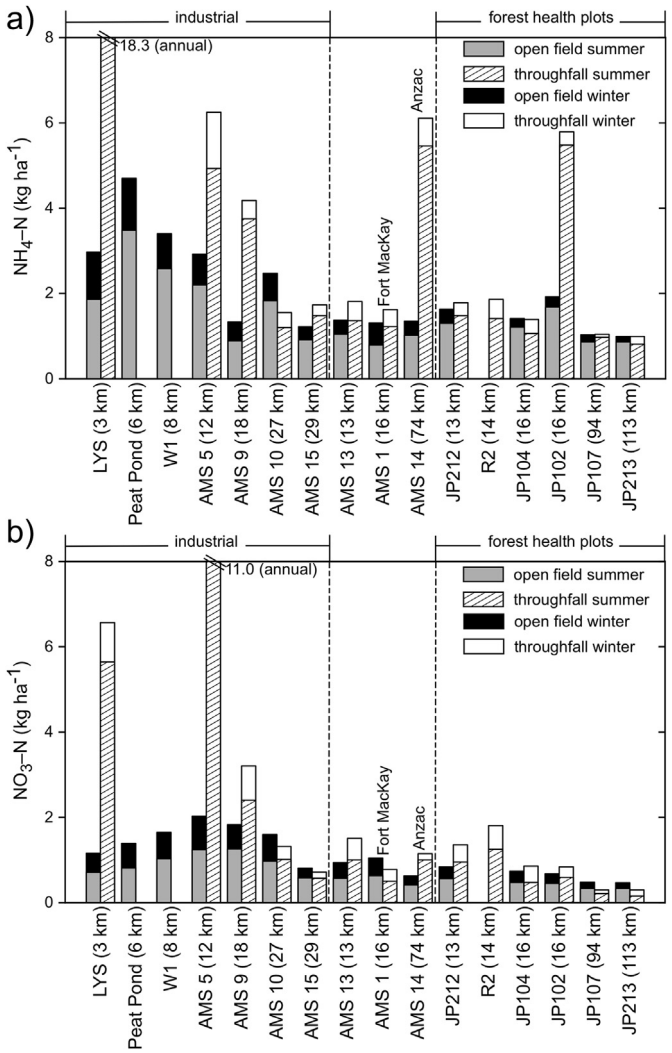

Fig. 2. Yearly deposition rates (May 2008 to May 2009) of NH_4–N (a) and NO_3–N (b) (averages for each sampling site) obtained for open field deposition and throughfall, divided into summer 2008 and winter 2008/2009 contributions. Forest health plots are typically more distant than industrial sites. AMS 1 (Fort MacKay) and AMS 14 (Anzac) are community sites.

Overall, $\delta^{15}N$–NH_4 values tended to be slightly higher in summer (−2.7 to +11.3‰) than in winter (−6.3 to +9.0‰). On average, deposition weighted mean values of $\delta^{15}N$–NH_4 for throughfall were 2‰ higher than the corresponding open field deposition $\delta^{15}N$–NH_4 values.

3.4. $\delta^{15}N$ of nitrate in atmospheric deposition

The NO_3–N-deposition-weighted, site-averaged nitrogen isotope ratios of atmospheric nitrate measured in open field deposition and throughfall are shown in Fig. 3b. Mean $\delta^{15}N$ values for open field deposition and throughfall ranged between −4.9 and +6.3‰. At distances >29 km predominantly negative $\delta^{15}N$ values were observed, particularly in the summer (1.1 to −4.4‰). At sites within 29 km distance of the emission stack more variable and also higher $\delta^{15}N$ values (up to +6.3‰) were observed. There was a shift of ~5‰ from lower $\delta^{15}N$ values during the summer sampling periods (average: −2.6 ± 2.0‰; range: −4.9 to +1.9‰) towards higher $\delta^{15}N$ values during the winter sampling periods (average: 2.1 ± 2.2‰; range: −2.0 to +6.3‰). For all sampling periods, the throughfall $\delta^{15}N$–NO_3 values were on average 1.2‰ higher ($\delta^{15}N$ values ranging between −3.8 and +6.3‰) than those of open field nitrate deposition (−4.9 and +4.7‰). The difference between throughfall and open field $\delta^{15}N$ values of nitrate was most pronounced in the summer 2008 sampling period when average $\delta^{15}N$–NO_3 values were almost 4‰ higher in throughfall samples compared to open field samples.

3.5. $\delta^{18}O$ of nitrate in atmospheric deposition

The NO_3–N-deposition-weighted, site-averaged $\delta^{18}O$–NO_3 values for open field deposition and throughfall ranged from 35.0 to 80.7‰. Lower $\delta^{18}O$ values of deposited nitrate (35.0–76.4‰) were observed within 29 km from the emission sources (Fig. 3c). More distant sites (>29 km) had $\delta^{18}O$ values of nitrate between 67.2 and 80.7‰. $\delta^{18}O$ values as low as 35.0‰ were only measured in close proximity (<18 km) to the emission stack. $\delta^{18}O$–NO_3 values lower than 56.8‰ were only observed during summer periods (Fig. 3c). On average, $\delta^{18}O$–NO_3 values in open field samplers were 3.6‰ higher than $\delta^{18}O$–NO_3 values in the corresponding throughfall samplers for the summer sampling periods, but $\delta^{18}O$–NO_3 values were similar (within 1‰) for both collector types during winter.

3.6. $\Delta^{17}O$ of nitrate in atmospheric deposition

The $\Delta^{17}O$ values of nitrate in open field samples ($n = 17$) and throughfall samples ($n = 13$) collected in summer 2007, winter 2007/2008, summer 2008 and winter 2008/2009 indicated non-zero $\Delta^{17}O$ values, and therefore mass-independent oxygen isotope fractionation. $\Delta^{17}O$ values ranged from 18.3 to 30.5‰ for open field samples and from 15.3 to 32.0‰ for throughfall samples (Fig. 3d). $\Delta^{17}O$ values lower than 20‰ were only observed within 12 km of the emission stack. Fig. 3d also indicates that $\Delta^{17}O$ values of nitrate deposited in winter are higher than those of summer deposition, on average by ~6‰.

4. Discussion

4.1. Nitrogen deposition in the AOSR

Our results show distinct spatial trends in atmospheric nitrate and ammonium deposition as a function of distance from the oil sands operations. Overall, nitrogen deposition rates in the AOSR are low compared to those from regions of North America, Asia and Europe that are influenced by elevated emissions from industry, agriculture or urbanized centers. In California, N deposition in areas more exposed to N emissions ranges from 15 to 70 kg N ha^{-1} yr^{-1} (Fenn et al., 2008, 2010). Considerable areas of Europe (MacDonald et al., 2002; Simpson et al., 2011) and the United States (Dentener et al., 2006) are exposed to N deposition as high as 15 kg N ha^{-1} yr^{-1} with hotspots receiving deposition levels of 20–30 kg N ha^{-1} yr^{-1} or greater (Fenn et al., 1998). In China bulk deposition (primarily wet deposition) averages 21.1 kg N ha^{-1} yr^{-1} (Liu et al., 2013). As expected, total N deposition values in China are much greater than bulk deposition, with peak values as high as 63 kg N ha^{-1} yr^{-1} in a national study (Lü and Tian, 2007); but deposition can be nearly double that amount in sites exposed to intensive agricultural and urban emissions (He et al., 2010).

The furthest distant sites JP107 (94 km) and JP213 (113 km) had annual open field and throughfall deposition rates of <1 kg ha^{-1} yr^{-1} and <0.5 kg ha^{-1} yr^{-1} for NH_4–N and NO_3–N, respectively. However, elevated annual deposition rates for NH_4–N (i.e. >>1 kg ha^{-1} yr^{-1}) and NO_3–N (i.e. >>0.5 kg ha^{-1} yr^{-1}) were observed in throughfall, particularly at industrial sites at 3 km, 12 km, 16 km, and 18 km distance from the emission stack (sites LYS,

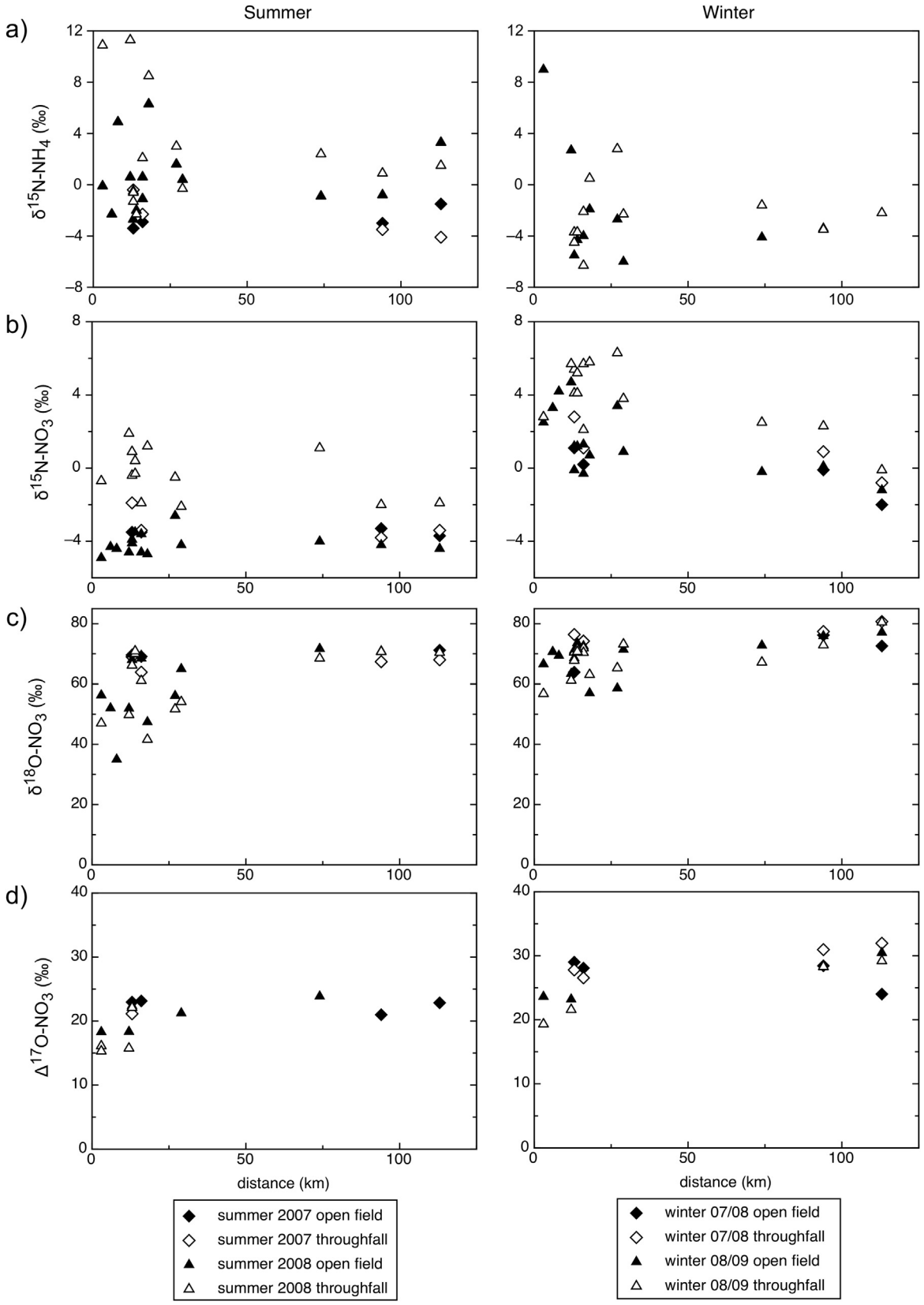

Fig. 3. Deposition-weighted, site-averaged $\delta^{15}N{-}NH_4$ (a), $\delta^{15}N{-}NO_3$ (b), $\delta^{18}O{-}NO_3$ (c) and $\Delta^{17}O{-}NO_3$ (d) values in open field deposition and throughfall versus distance from the emission stack for the summer periods (left) and winter periods (right).

AMS 5, JP102 and AMS 9). This indicates that dry deposition accumulated on tree canopies is subsequently washed off, making it a major contributor to N deposition in the vicinity of the oil sands operations. NH_4–N in throughfall exceeded 18 kg ha^{-1} yr^{-1} at the industrial site LYS, the site closest to the emission stack (3 km). The highest NO_3–N deposition rate was observed in throughfall at the industrial site AMS 5 (11 kg ha^{-1} yr^{-1}, 12 km), a site close to open pit mining and the major highway (Hwy 63) that connects Fort McMurray with the oil sands operations. Overall, NH_4–N deposition rates are higher than NO_3–N deposition rates except for one throughfall (AMS 5) and one open field sampling site (AMS 9), making NH_4 the dominant contributor to nitrogen deposition in the AOSR. NH_4–N deposition rates were highest near one of the major emission stacks. High atmospheric NH_3 gas concentrations have been reported for the AOSR (Bytnerowicz et al., 2010) suggesting that industrial activities are responsible for elevated ammonia concentrations and hence ammonium deposition in the AOSR. Agricultural emissions can be excluded in the AOSR, but significant NH_3 emissions have been reported for vehicle engines equipped with three-way catalytic converters (Bishop et al., 2010; Fraser and Cass, 1998). Open pit mining in the AOSR is accomplished with heavy haulers powered by diesel engines. Proemse et al. (2012a) estimated that the overall annual fuel consumption of heavy haulers exceeds 538 million L of diesel yielding 16,700 t of NO_x per year. Stack released gaseous NO_2 and NH_3 emissions from the main oil sand operations were 26,848 t and 587 t respectively for 2009 (NPRI, 2011). If these emissions data are approximately correct, NH_3 stack emissions alone cannot account for ammonium deposition rates that typically exceed nitrate deposition rates. This suggests that emission monitoring in the AOSR is either insufficient or there is an unidentified or under-reported source of NH_3. In throughfall, the greater deposition of reduced N could be partially due to the higher deposition velocity of NH_3 compared to NO_2. Nitric acid vapor (HNO_3) has a similar deposition velocity to that of NH_3, but atmospheric concentrations of HNO_3 vapor in the AOSR are generally much lower than concentrations of NH_3 (Bytnerowicz et al., 2010).

4.2. Nitrogen isotope ratios of ammonium and nitrate

Nitrogen isotope ratios of ammonium and nitrate may provide information about sources of atmospheric nitrogen. Elevated deposition-weighted, site-averaged $\delta^{15}N$–NH_4 values of up to +11.3‰ were observed within 18 km of the oil sands operations. Fig. 4a shows that elevated $\delta^{15}N$–NH_4 values were generally associated with elevated NH_4–N deposition rates (=low values for 1/(NH_4–N)). Proemse et al. (2012a) recently reported $\delta^{15}N$ values of ammonium in $PM_{2.5}$ (particulate matter with <2.5 μm diameter) emitted from one of the stacks in the oil sands region, having $\delta^{15}N$ values of up to +20.1‰. In contrast, samples with NH_4–N deposition rates <0.5 kg N ha^{-1} (1/(NH_4–N) ≈ 2) had an average $\delta^{15}N$–NH_4 value of −3.6 ± 0.9‰ during summer and of −3.2 ± 2.2‰ during winter (horizontal gray boxes in Fig. 4a). $\delta^{15}N$–NH_3 values as low as −10.0 ± 2.6‰ have been reported by Moore (1977) for less polluted air as a result of natural soil emissions, suggesting that the negative $\delta^{15}N$ values for NH_4 observed at sites with low NH_4–N deposition rates indicate contributions from non-industrial ammonium sources. The difference between low $\delta^{15}N$–NH_4 values at sites with low NH_4–N deposition rates and elevated $\delta^{15}N$–NH_4 values at sites close to the oil sands operations in the AOSR make it feasible to use nitrogen isotope ratios to estimate industrial contributions to atmospheric ammonium deposition. One current limitation is that no $\delta^{15}N$–NH_4 values were determined or are known for vehicle exhaust and other possible NH_3 sources for this region.

$\delta^{15}N$–NH_4 values reported in the literature are typically lower than $\delta^{15}N$–NO_3 values in atmospheric deposition, due to the fact that natural NH_3 is often depleted in ^{15}N (Kendall, 1998; Garten, 1992; Heaton, 1986). In contrast, we observed higher $\delta^{15}N$–NH_4 than $\delta^{15}N$–NO_3 values during summer at sites with elevated N deposition rates (Fig. 3a, b), providing a potential tracer of industrial emissions that is also accumulated in bio-indicators (Proemse and Mayer, 2012). Similar observations have been made for nitrogen deposition in Boulder, Colorado (Moore, 1977). Furthermore, Moore (1977) reported ^{15}N enrichment for both NO_3 and NH_4 in particulates compared to $\delta^{15}N$ values in rainfall. This is consistent with our data that show slightly higher $\delta^{15}N$–NH_4 values and higher NH_4 deposition rates in throughfall samples (Fig. 3a), likely related to dry deposition of NH_4 particles enriched in ^{15}N in the forest canopy (Heaton et al., 1997; Garten, 1992).

Fig. 4b shows that elevated $\delta^{15}N$ values in atmospheric nitrate deposition were also associated with elevated NO_3–N deposition rates (=low values for 1/(NO_3–N)). Stack emitted nitrate in $PM_{2.5}$ from one of the oil sand operations in the AOSR had an average $\delta^{15}N$–NO_3 value of 16.1 ± 1.2‰ (n = 6) (Proemse et al., 2012a). Particulate matter does not represent the largest fraction of stack emitted nitrogen from the oil sands operations, but elevated $\delta^{15}N$ values as high as 21‰ were also recently reported for gaseous NO_x emissions from coal-fired power plants in the northeastern and midwestern US (Felix et al., 2012), suggesting that industrial nitrogen emissions are associated with elevated $\delta^{15}N$ values. This is supported by the observation that elevated $\delta^{15}N$ values of atmospheric nitrate deposited in the AOSR mostly occur within a 29 km radius of the emission stack (Fig. 3b). Deposition-weighted, site-averaged $\delta^{15}N$ values of atmospheric nitrate in winter as high as +6.3‰ (Fig. 3b) suggest that industrial nitrogen is a contributor to atmospheric nitrate in the vicinity of industrial emitters in the AOSR. Background atmospheric nitrate, indicated by samples with NO_3–N deposition rates <0.1 kg N ha^{-1} (1/(NO_3–N) ≈ 10) had an average $\delta^{15}N$–NO_3 value of −3.2 ± 1.5‰ during summer and 0.3 ± 1.7‰ during winter (horizontal gray box in Fig. 4b).

Seasonal variations of $\delta^{15}N$ of nitrate in atmospheric deposition with higher values during winter have been observed previously (Elliott et al., 2007; Freyer, 1991). This may be caused by elevated natural nitrogen emissions during summer having lower $\delta^{15}N$ values due to biogenic processes. Freyer (1991) proposed that higher $\delta^{15}N$–NO_3 values in winter are due to increased fossil fuel combustion. Our data show that N deposition rates are highest during the summer months (Fig. 4b) as a result of higher precipitation rates compared to winter, but $\delta^{15}N$ values of nitrate were elevated during the winter periods. Throughfall $\delta^{15}N$–NO_3 values were usually higher than corresponding open field deposition $\delta^{15}N$–NO_3 values. This indicates that dry deposition likely associated with industrial particles with high $\delta^{15}N$ values (Proemse et al., 2012a) may be significant, particularly during the winter when wet deposition is low (Proemse et al., 2012b).

4.3. Oxygen isotope ratios of nitrate

Oxygen isotope ratios of nitrate may reveal additional information about sources and processes occurring in the atmospheric N cycle. Anomalous enrichment of ^{17}O and ^{18}O in nitrate is due to oxidation of NO_x ($NO + NO_2$) via oxygen transfer of ozone (O_3). The $\Delta^{17}O$ anomaly in ozone is well known (Thiemens and Heidenreich, 1983) and has been widely used to understand atmospheric oxidation pathways and sources of nitrate (Michalski et al., 2004; Savarino et al., 2007), although its origin is still debated today (Michalski and Bhattacharya, 2009).

Both $\Delta^{17}O$ and $\delta^{18}O$ values measured in atmospheric nitrate deposition in the AOSR are typically higher in the winter compared to summer values (Fig. 4c, d), indicating a change in atmospheric oxidation pathways. There are two homogenous reactions

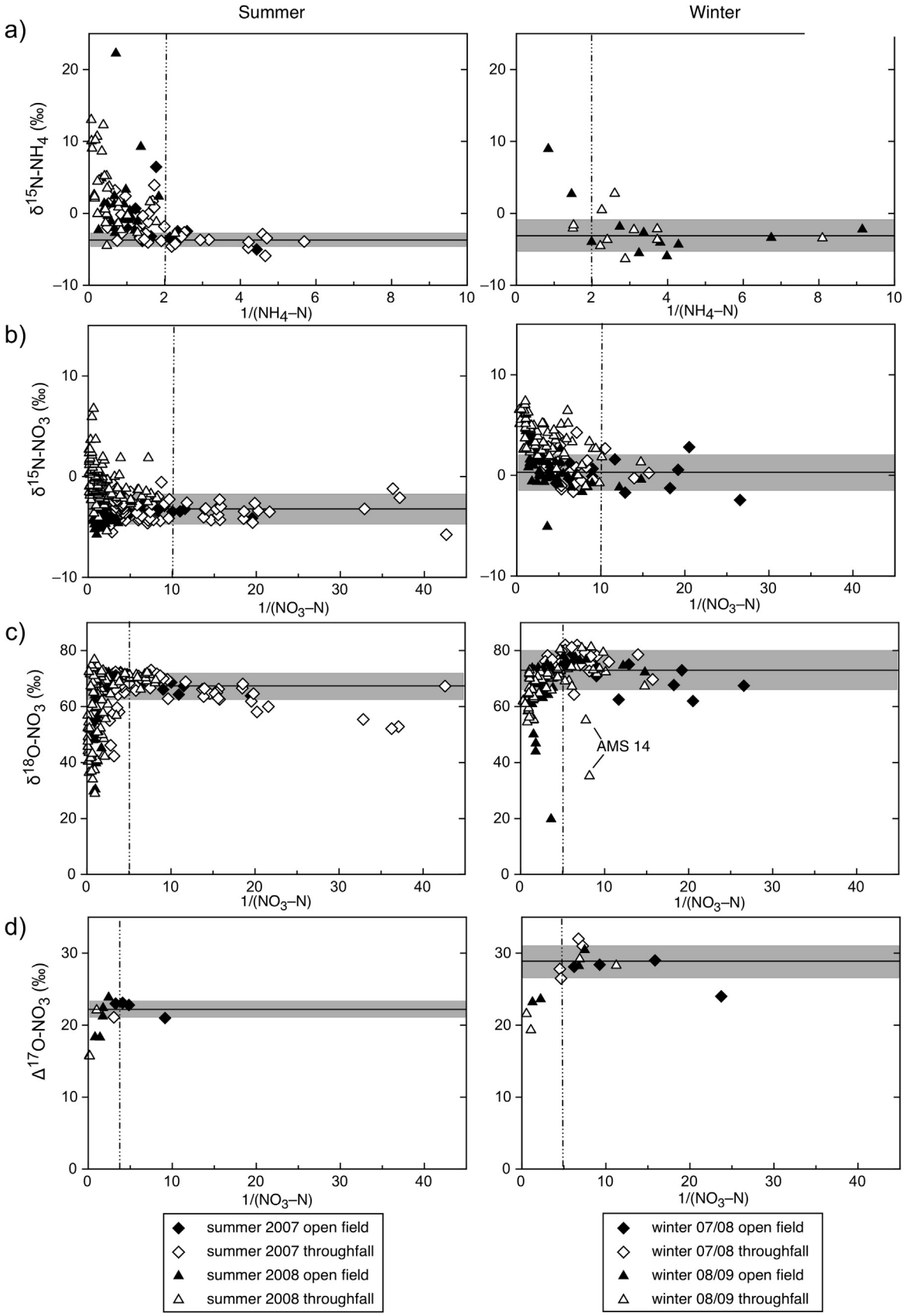

Fig. 4. (a) $\delta^{15}N-NH_4$, (b) $\delta^{15}N-NO_3$, (c) $\delta^{18}O-NO_3$ and (d) $\Delta^{17}O-NO_3$ values in open field deposition and throughfall samples versus 1 over deposition rates (1/(kg ha^{-1})) for the summer periods (left) and winter periods (right). Horizontal lines indicate mean values of isotope ratios and their standard deviations (gray shaded area) for samples with low NO_3–N deposition rates (samples to the right of the vertical dotted lines).

(Equations (3) and (4)) and one heterogeneous reaction (Equation (5)) that form atmospheric nitrate ($NO_3 + HNO_3$) from NO_2 (Michalski et al., 2003):

$$NO_2 + OH + M \rightarrow HNO_3 + M \quad (3)$$

$$NO_2 + O_3 \rightarrow NO_3 + O_2 \quad (4)$$

$$NO_2 + NO_3 \leftrightarrow N_2O_5,\ N_2O_5 + H_2O\ (\text{surface}) \rightarrow 2\ HNO_3\ (\text{aq}) \quad (5)$$

The oxidation via ozone (Equation (4)) predominantly occurs during winter (Morin et al., 2008; Michalski et al., 2003; Hastings et al., 2003) resulting in higher $\Delta^{17}O$ and $\delta^{18}O$ values due to interaction with ozone. Tropospheric OH does not possess an anomalous enrichment of ^{17}O due to rapid oxygen exchange with H_2O, hence $\Delta^{17}O$ of OH is ~0‰ (Lyons, 2001), whereas tropospheric O_3 at mid-latitudes has $\Delta^{17}O$ values of ~35‰ (Michalski et al., 2004), resulting in $\Delta^{17}O$ values of ~20–31‰ for atmospheric nitrate deposition (Michalski et al., 2003). Consistent with these literature data, atmospheric nitrate in the AOSR with NO_3–N deposition rates <0.2 kg ha^{-1} ($1/(NO_3\text{–}N) \approx 5$) had average $\Delta^{17}O$ values of 22.2 ± 1.1‰ during summer and 28.9 ± 2.2‰ during winter (Fig. 4d). With increasing NO_3–N deposition rates (>0.2 kg ha^{-1}), however, a trend towards lower $\Delta^{17}O$ values of ~15‰ for summer and ~20‰ for winter was observed (Fig. 4d). The lowest $\Delta^{17}O$ values were found at sites <12 km from the emission sources that were characterized by the highest nitrate deposition rates (Figs. 3d and 4d). Stack emitted nitrate in $PM_{2.5}$ from one of the oil sands facilities had $\Delta^{17}O$ values close to zero (0.5 ± 0.9‰, $n = 5$) (Proemse et al., 2012a). We therefore suggest that industrial derived nitrate characterized by negligible mass-independent isotope fractionation for ^{17}O causes atmospheric nitrate deposition with low $\Delta^{17}O$ values. The discrepancy between near zero $\Delta^{17}O$ values of directly emitted particulate nitrate and higher $\Delta^{17}O$ values of nitrate affected by industrial deposition emissions may be due to oxygen isotopic equilibrium reactions of gaseous NO_x with ozone prior to its conversion to nitrate (Alexander et al., 2009). Since it is expected that NO_3 derived via long-range transport is anomalously enriched in oxygen-17 due to rapid oxygen exchange with ozone, we conclude that the $\Delta^{17}O$ values as low as 15.3‰ observed in atmospheric nitrate deposition samples close to the emission stack are indicative of industrial nitrogen contributions to atmospheric nitrate deposition. This is likely due to dominant hydroxyl radical (OH) oxidation close to the emission sources. This has often been observed in emission plumes from stacks and may be associated with NO_x emissions (Lawrence and Crutzen, 1999) or HO_2 radical production during CO_2 formation that subsequently oxidize NO emissions according to Seinfeld and Pandis (2006)

$$HO_2 + NO \rightarrow NO_2 + OH \quad (6)$$

This reaction terminates in the formation of nitric acid according to Equation (3).

Fig. 4c shows that lower $\delta^{18}O$ values in atmospheric nitrate deposition were generally associated with elevated NO_3–N deposition rates, regardless of the season, whereas the highest $\delta^{18}O$ values were associated with lowest NO_3–N deposition rates (=high $1/(NO_3\text{–}N)$). Samples of atmospheric nitrate deposition with NO_3–N deposition rates <0.2 kg ha^{-1} ($1/(NO_3\text{–}N) \approx 5$), had average $\delta^{18}O$–NO_3 values of 67.4 ± 4.4‰ during summer and 73.0 ± 7.4‰ during winter (Fig. 4c). Our deposition-weighted, site-averaged $\delta^{18}O$–NO_3 values observed within 32 km distance to the oil sand operations were as low as ~35‰ during the summer, lower than $\delta^{18}O$ values typically reported for atmospheric nitrate deposition ranging from ~60 to ~95‰ (Kendall et al., 2007 and references therein). Nitrate in $PM_{2.5}$ emitted from a major stack in the AOSR had low $\delta^{18}O$ values averaging 17.6 ± 1.8‰ ($n = 6$) (Proemse et al., 2012a) suggesting that low $\delta^{18}O$ values in atmospheric nitrate deposition are indicative of industrial nitrate contributions. Similarly, low oxygen isotope ratios in atmospheric nitrate deposition were reported by Fang et al. (2011) for a N-polluted city in China, indicating that low $\delta^{18}O$–NO_3 values constitute a valuable tracer of anthropogenic atmospheric nitrate.

4.4. Estimation of industrially derived nitrate in atmospheric nitrate deposition

Stack emitted nitrate in $PM_{2.5}$ from one of the operators in the AOSR had markedly lower $\delta^{18}O$ and $\Delta^{17}O$ values (Proemse et al., 2012a) compared to nitrate deposition at distant forest health plots. When $\delta^{18}O$ and $\Delta^{17}O$ values for industrial emissions and for background nitrate (e.g. from long-range transport) are known and different, a two-end-member mixing model can be used to determine industrial contributions to atmospheric nitrate deposition in the AOSR, similar to the approach used to estimate industrial contributions to atmospheric sulfate deposition in the AOSR (Proemse et al., 2012b). The fraction f of industrially derived nitrate contributing to the total nitrate deposition can be resolved applying a two-end-member mixing model:

$$\delta^{18}O_M = f\delta^{18}O_{STACK} + (1-f)\delta^{18}O_{BGRD} \quad (7)$$

yielding

$$f = \left(\delta^{18}O_M - \delta^{18}O_{BGRD}\right) \Big/ \left(\delta^{18}O_{STACK} - \delta^{18}O_{BGRD}\right) (0 < f < 1) \quad (8)$$

where $\delta^{18}O_M$ is the oxygen isotopic composition of the mixture (deposition-weighted, site-averaged values), $\delta^{18}O_{STACK}$ and $\delta^{18}O_{BGRD}$ the oxygen isotopic compositions of the emission stack nitrate and the background atmospheric nitrate, respectively. The same equations can be applied to $\Delta^{17}O$ values with $\Delta^{17}O_{STACK}$ and $\Delta^{17}O_{BGRD}$. Since the oxygen isotopic composition of atmospheric nitrate depends on its oxidation pathway, which also varies with season, calculations with different background values were conducted for summer and winter separately. For stack nitrate, $\Delta^{17}O_{STACK}$ and $\delta^{18}O_{STACK}$ average values of 0.5 and 17.6‰ were used, respectively (Proemse et al., 2012a). Applying these low values for $\Delta^{17}O_{STACK}$ and $\delta^{18}O_{STACK}$ results in underestimation of industrial nitrate contributions because some industrial derived NO_x may react with ozone in the atmosphere during the oxidation to NO_3 and hence may have more elevated oxygen isotope ratios. Calculations therefore represent minimum industrial contributions. $\delta^{18}O$ and $\Delta^{17}O$ values for gaseous nitrogen emissions and vehicle emissions have not been determined, but similar low values as found in $PM_{2.5}$ (Proemse et al., 2012a) can be expected due to the absence of ozone until the release of NO_x from the stacks. $\Delta^{17}O_{BGRD}$ and $\delta^{18}O_{BGRD}$ values of 22.2‰ and 67.4‰ for summer, and 28.9 and 73.0‰ for winter, respectively, were used, based on mean values for sites with low NO_3–N deposition rates (Fig. 4c, d). Calculated minimum industrial contributions to atmospheric nitrate deposition in the AOSR are summarized in Table 1 and vary between 0 and 65% depending on the site location (Fig. 5). Fig. 5 also shows that minimum industrial contributions to nitrate deposition are similar spatially distributed as minimum industrial contributions to sulfate deposition (Proemse et al., 2012b). Minimum industrial contributions to atmospheric nitrate deposition at forest health plots were <8.3% during all four sampling periods (Table 1). The community sites AMS 1 (Fort McKay) and AMS 14 (Anzac) as well as AMS 13

Table 1
Summary of atmospheric nitrate and ammonium deposition rates for the sampling sites investigated over all four sampling periods and their isotopic composition (in ‰). Deposition-weighted, site-averaged values are reported for $\delta^{18}O-NO_3$ and $\delta^{15}N-NH_4$.Minimum industrial contributions to atmospheric nitrate deposition estimated by two-end-member mixing calculations using $\Delta^{17}O-NO_3$ values and deposition-weighted, site-averaged $\delta^{18}O-NO_3$ values of open field deposition and throughfall for all four sampling periods are shown (in %). Deposition-weighted, site-averaged $\delta^{15}N-NH_4$ values were used to estimate the reported industrial contributions to atmospheric ammonium deposition in the AOSR.

Site	Type	Distance (km)	NH_4-N (kg/ha)	NO_3-N (kg/ha)	$\Delta^{17}O-NO_3$ (‰)	$\delta^{15}N-NO_3$ (‰)	$\delta^{18}O-NO_3$ (‰)	$\delta^{15}N-NH_4$ (‰)	Industrial NH_4 using $\delta^{15}N$ (%)	Industrial NO_3 using $\delta^{18}O$ (%)	Industrial NO_3 using $\Delta^{17}O$ (%)
Summer 2007											
JP212	Open field	13	0.61	0.31	23.0	−3.5	69.6	−3.4	1	0[a]	0[a]
JP212	Throughfall	13	0.88	0.33	21.1	−1.9	69.0	−0.4	19	0[a]	5
JP102	Open field	16	0.61	0.24	23.1	−3.5	69.1	−2.9	4	0[a]	0[a]
JP102	Throughfall	16	0.95	0.25	n.d.	−3.4	63.9	−2.3	8	7	
JP107	Open field	94	0.24	0.11	21.0	−3.3	67.3	−3.0	3	0	6
JP107	Throughfall	94	0.34	0.10	n.d.	−3.8	67.4	−3.5	1	0	
JP213	Open field	113	0.51	0.21	22.8	−3.7	71.2	−1.5	13	0[a]	0[a]
JP213	Throughfall	113	0.18	0.07	n.d.	−3.4	68.0	−4.1	0[a]	0[a]	
Winter 2007/2008											
JP212	Open field	13	0.03	0.06	29.0	1.1	63.9	n.d.		16	0[a]
JP212	Throughfall	13	0.08	0.22	27.8	2.8	76.4	n.d.		0[a]	4
JP102	Open field	16	0.18	0.16	28.1	0.2	74.3	n.d.		0[a]	3
JP102	Throughfall	16	0.16	0.21	26.5	1.1	74.2	n.d.		0[a]	8
JP107	Open field	94	0.08	0.11	28.4	−0.1	76.2	n.d.		0[a]	2
JP107	Throughfall	94	0.10	0.14	31.0	0.9	77.4	n.d.		0[a]	0[a]
JP213	Open field	113	0.03	0.04	24.0	−2.0	72.6	n.d.		1	17
JP213	Throughfall	113	0.12	0.15	32.0	−0.8	80.7	n.d.		0[a]	0[a]
Summer 2008											
LYS	Open field	3	1.86	0.71	18.3	−4.9	56.3	−0.1	21	22	18
LYS	Throughfall	3	14.90	5.64	15.7	−0.7	47.0	10.9	87	41	30
Peat Pond	Open field	6	3.48	0.81	n.d.	−4.3	52.0	−2.3	8	31	
W1	Open field	8	2.58	1.03	n.d.	−4.4	35.0	4.9	51	65	
AMS 5	Open field	12	2.20	1.24	18.4	−4.6	51.9	0.6	25	31	18
AMS 5	Throughfall	12	4.93	9.18	15.8	1.9	49.8	11.3	90	35	30
AMS 13	Open field	13	1.04	0.57	22.4	−4.1	68.0	−0.5	19	0[a]	0[a]
AMS 13	Throughfall	13	1.36	1.00	22.1	0.9	66.2	−0.6	18	2	0
JP212	Open field	13	1.30	0.56	n.d.	−3.9	69.8	−2.7	5	0[a]	
JP212	Throughfall	13	1.48	0.95	n.d.	−0.4	66.2	−1.3	14	2	
R2	Throughfall	14	1.41	1.25	n.d.	0.4	70.9	−4.5	0[a]	0[a]	
JP104	Open field	14	1.21	0.47	n.d.	−3.5	70.0	−2.0	9	0[a]	
JP104	Throughfall	14	1.06	0.47	n.d.	−0.3	70.0	−2.3	8	0[a]	
AMS 1	Open field	16	0.79	0.63	n.d.	−3.6	69.4	0.6	25	0[a]	
AMS 1	Throughfall	16	1.22	0.50	n.d.	n.d.	n.d.	n.d.			
JP102	Open field	16	1.68	0.45	n.d.	−4.6	68.5	−1.1	15	0[a]	
JP102	Throughfall	16	5.48	0.59	n.d.	−1.9	61.1	2.1	34	13	
AMS 9	Open field	18	0.89	1.26	n.d.	−4.7	47.4	6.3	60	40	
AMS 9	Throughfall	18	3.75	2.40	n.d.	1.2	41.6	8.5	73	52	
AMS 10	Open field	27	1.83	0.97	n.d.	−2.6	56.1	1.6	32	23	
AMS 10	Throughfall	27	1.20	1.01	n.d.	−0.5	51.7	3.0	40	31	
AMS 15	Open field	29	0.91	0.58	21.2	−4.2	65.0	0.4	24	5	4
AMS 15	Throughfall	29	1.48	0.57	n.d.	−2.1	54.1	−0.3	20	27	
AMS 14	Open field	74	1.02	0.41	23.9	−4.0	71.7	−0.9	16	0[a]	0[a]
AMS 14	Throughfall	74	5.46	1.00	n.d.	1.1	68.5	2.4	36	0[a]	
JP107	Open field	94	0.86	0.33	n.d.	−4.2	70.9	−0.8	17	0[a]	
JP107	Throughfall	94	0.97	0.21	n.d.	−2.0	70.7	0.9	27	0[a]	
JP213	Open field	113	0.86	0.33	n.d.	−4.4	70.5	3.3	42	0[a]	
JP213	Throughfall	113	0.81	0.15	n.d.	−1.9	70.4	1.5	31	0[a]	
Winter 2008/2009											
LYS	Open field	3	1.11	0.45	23.6	2.5	66.6	9.0	75	12	19
LYS	Throughfall	3	3.36	0.93	19.3	2.8	56.8	n.d.		29	34
Peat Pond	Open field	6	1.22	0.58	n.d.	3.3	70.7	n.d.		4	
W1	Open field	8	0.82	0.62	n.d.	4.2	69.4	n.d.		7	
AMS 5	Open field	12	0.72	0.79	23.2	4.7	63.4	2.7	36	17	20
AMS 5	Throughfall	12	1.32	1.83	21.6	5.7	61.2	n.d.		21	26
AMS 13	Open field	13	0.32	0.37	n.d.	−0.1	68.6	−5.5	0[a]	8	
AMS 13	Throughfall	13	0.45	0.51	n.d.	4.1	67.8	−4.5	0[a]	9	
JP212	Open field	13	0.33	0.28	n.d.	1.2	71.1	n.d.		3	
JP212	Throughfall	13	0.29	0.42	n.d.	5.4	70.5	−3.7	0[a]	4	
R2	Throughfall	14	0.45	0.55	n.d.	5.2	70.7	n.d.		4	
JP104	Open field	14	0.21	0.27	n.d.	1.2	73.6	−4.3	0[a]	0[a]	
JP104	Throughfall	14	0.33	0.39	n.d.	4.1	71.6	−3.7	0[a]	3	
AMS 1	Open field	16	0.51	0.42	n.d.	1.3	72.1	−4.0	0[a]	2	
AMS 1	Throughfall	16	0.40	0.28	n.d.	5.7	71.9	−2.1	7	2	
JP102	Open field	16	0.24	0.23	n.d.	−0.3	72.6	n.d.		1	
JP102	Throughfall	16	0.30	0.25	n.d.	2.1	70.4	−6.3	0[a]	5	
AMS 9	Open field	18	0.44	0.57	n.d.	0.7	57.0	−1.9	8	29	
AMS 9	Throughfall	18	0.42	0.81	n.d.	5.8	63.1	0.5	23	18	

Table 1 (*continued*)

Site	Type	Distance (km)	NH_4–N (kg/ha)	NO_3–N (kg/ha)	$\Delta^{17}O$–NO_3 (‰)	$\delta^{15}N$–NO_3 (‰)	$\delta^{18}O$–NO_3 (‰)	$\delta^{15}N$–NH_4 (‰)	Industrial NH_4 using $\delta^{15}N$ (%)	Industrial NO_3 using $\delta^{18}O$ (%)	Industrial NO_3 using $\Delta^{17}O$ (%)
AMS 10	Open field	27	0.63	0.63	n.d.	3.4	58.6	−2.7	3	26	
AMS 10	Throughfall	27	0.35	0.30	n.d.	6.3	65.3	2.8	37	14	
AMS 15	Open field	29	0.31	0.23	n.d.	0.9	71.4	−6.0	0[a]	3	
AMS 15	Throughfall	29	0.24	0.16	n.d.	3.8	73.2	−2.3	6	0[a]	
AMS 14	Open field	74	0.33	0.22	n.d.	−0.2	72.8	−4.1	0[a]	0	
AMS 14	Throughfall	74	0.65	0.15	n.d.	2.5	67.2	−1.6	10	10	
JP107	Open field	94	0.17	0.15	28.2	0.1	75.9	−3.4	0[a]	0[a]	2
JP107	Throughfall	94	0.07	0.09	28.3	2.3	72.9	−3.5	0[a]	0	2
JP213	Open field	113	0.13	0.13	30.5	−1.2	77.1	−2.2	6	0[a]	0[a]
JP213	Throughfall	113	0.18	0.15	29.2	−0.1	80.5	−2.2	6	0[a]	0[a]

n.d. = not determined (e.g. due to too low concentrations or insufficient material).
[a] Negative results were set to zero.

appear to be little affected by industrial nitrate contributions (<10.4%). Nitrate deposition with >25% industrially derived N was only observed at industrial sites. The highest minimum industrial contribution to atmospheric nitrate deposition of 65% was observed at the industrial site W1, 8 km from one of the emission stacks. Fig. 5 shows that calculated minimum industrial contributions to nitrate deposition are highest at industrial sites within 29 km. In contrast, atmospheric nitrate deposition at sites >90 km from the main emission sources does not appear to be affected by significant contributions of industrially derived nitrate. On average, estimates of industrial nitrate contributions using $\delta^{18}O$ and $\Delta^{17}O$ values differ by <5%, suggesting that both parameters are suitable for this purpose. The difference may be due to the fact that average site values were used for $\delta^{18}O$, but only measurements of individual samples were available for $\Delta^{17}O$ values. Choosing a different $\Delta^{17}O_{STACK}$ value of 1.8‰ (highest value observed for stack $PM_{2.5}$ nitrate, Proemse et al., 2012a) affects results on average by <0.6%.

4.5. Estimation of industrially derived ammonium in atmospheric ammonium deposition

The same approach as described above can be applied using $\delta^{15}N$–NH_4 values to estimate industrial contributions to atmospheric ammonium deposition. Although a wide range of $\delta^{15}N$ values was observed for NH_4 in $PM_{2.5}$ emissions (Proemse et al., 2012a), we observed a trend towards higher $\delta^{15}N$ values at atmospheric deposition sites with high NH_4–N deposition rates. The highest ammonium deposition rate of 17.6 kg ha^{-1} (summer 2008) was observed at the site (LYS) closest to one of the major oil sands operations (3 km) and was associated with a $\delta^{15}N$–NH_4 value of 13.0‰. Using this $\delta^{15}N$ value as the end-member for industrial emissions of reduced nitrogen, and the $\delta^{15}N$–NH_4 values for summer (−3.6‰) and winter (−3.2‰) sampling periods at low deposition sites (<0.5 kg ha^{-1} yr^{-1}, Fig. 4a) for non-industrially derived ammonium, industrial contributions to NH_4 deposition can be calculated using approaches similar to those outlined in Equations 7 and 8. Estimated industrial contributions to atmospheric ammonium deposition in the AOSR are summarized in Table 1 and vary between 0 and 90% depending on the site location. Industrial contributions to atmospheric ammonium deposition were highest on industrial sites, but also the furthest distant site (JP213, 113 km) appears to be significantly affected by industrial contributions (Fig. 5). This is consistent with the observation that ammonium deposition typically exceeds nitrate deposition in the AOSR. However, this preliminary approach assumes that there are no other sources of atmospheric ammonium in the AOSR and that the $\delta^{15}N$ value of +13.0‰ is representative for industrial ammonium emissions from all oil sands operators. Hence, further characterization of emission sources of ammonium is required especially since source apportionment calculations are very sensitive to the choice of $\delta^{15}N$ values of end-members. For instance, a 3‰ variation in the $\delta^{15}N$ value of the industrial source signal would lead to differences in industrial contributions to atmospheric ammonium deposition of up to 20%.

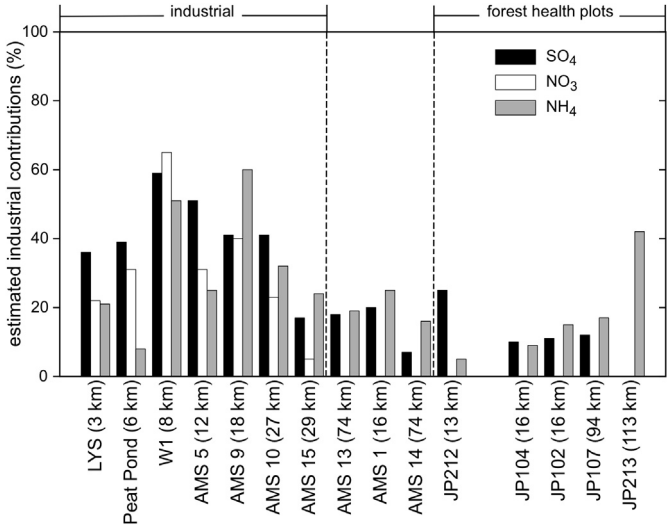

Fig. 5. Minimum industrial contributions estimated using two-end-member mixing calculations to atmospheric nitrate compared to sulfate deposition (Proemse et al., 2012b), using $\delta^{18}O$–NO_3 values for open field samples exposed in summer 2008. $\delta^{15}N$–NH_4 values were used to estimate industrial contributions to ammonium deposition that typically exceeds nitrate deposition in the AOSR.

5. Conclusions

Nitrogen deposition is low at forest health plots in the AOSR but elevated at industrial sampling sites within ~30 km distance to the major operations, especially in throughfall samplers. Dry deposition washed off from the tree canopy was identified as an important contributor to total N deposition in the AOSR. NH_4–N deposition typically exceeded NO_3–N deposition, although the cause for this observation remains ambiguous. Stable isotope techniques were successfully applied to estimate industrial contributions to nitrate and ammonium deposition in the AOSR. Elevated $\delta^{15}N$ values in nitrate and ammonium deposition observed within ~30 km radius to the oil sands operations are indicative of industrial N contributions. Both $\Delta^{17}O$ and $\delta^{18}O$ of atmospheric nitrate allowed for the estimation of minimum industrial contributions to nitrate deposition. Data for forest health plots and community sites revealed low

minimum contributions (typically less than 5%) of industrially derived nitrogen, whereas industrial sites were significantly influenced (>>10% up to 65%) by industrially derived nitrogen. A similar approach using $\delta^{15}N$ values of ammonium revealed significant industrial contributions to ammonium deposition sites in close proximity to the main emission sources in the AOSR, but additional characterization of emission sources of ammonium is required to further refine this tracer approach. We conclude that distinct patterns of oxygen and nitrogen isotope ratios in atmospheric nitrate and ammonium deposition can be used to estimate industrially derived nitrogen contributions to atmospheric N deposition in the Athabasca oil sands region.

Acknowledgments

This study was funded by the Wood Buffalo Environmental Association (WBEA), the Natural Sciences and Engineering Research Council of Canada (NSERC CRDPJ 372151-08), and the Canada School for Energy and the Environment (CSEE). We thank the staff of WBEA for their assistance in project coordination and for obtaining samples, in particular Veronica Chisholm and Kevin Percy. We also thank IsoLab at the University of Washington, Seattle, for conducting $\Delta^{17}O$ analyses and Stephen Taylor and the staff from the Isotope Science Laboratory (ISL) at the University of Calgary for their help with $\delta^{15}N$ and $\delta^{18}O$ analyses.

References

Alexander, B., Hastings, M., Allman, D., Dachs, J., Thornton, J., Kunasek, S., 2009. Quantifying atmospheric nitrate formation pathways based on a global model of the oxygen isotopic composition ($\Delta^{17}O$) of atmospheric nitrate. Atmospheric Chemistry and Physics 9, 5043–5056.

AMEC, 2001. Jack Pine Acid Deposition Monitoring Network Site Selection 2000. Wood Buffalo Environmental Association, CE02078, AMEC Earth & Environment Limited, Calgary, Alberta, Canada, p. 51.

Ammann, M., Siegwolf, R., Pichlmayer, F., Suter, M., Saurer, M., Brunold, C., 1999. Estimating the uptake of traffic-derived NO_2 from ^{15}N abundance in Norway spruce needles. Oecologia 118, 124–131.

Bishop, G.A., Peddle, A.M., Stedman, D.H., Zhan, T., 2010. On-road emission measurements of reactive nitrogen compounds from three California cities. Environmental Science & Technology 44, 3616–3620.

Bytnerowicz, A., Fraczek, W., Schilling, S., Alexander, D., 2010. Spatial and temporal distribution of ambient nitric acid and ammonia in the Athabasca oil sands region, Alberta. Journal of Limnology 69, 11–21.

Casciotti, K.L., Sigman, D.M., Hastings, M.G., Böhlke, J.K., Hilkert, A., 2002. Measurement of the oxygen isotopic composition of nitrate in seawater and freshwater using the denitrifier method. Analytical Chemistry 74, 4905–4912.

Cheng, Y., Cai, Z.-C., Zhang, J.-B., Chang, S.X., 2011. Gross N transformations were little affected by 4 years of simulated N and S depositions in an aspen-white spruce dominated boreal forest in Alberta, Canada. Forest Ecology and Management 262, 571–578.

Dentener, F., Drevet, J., Lamarque, J.F., Bey, I., et al., 2006. Nitrogen and sulfur deposition on regional and global scales: a multimodel evaluation. Global Biogeochemical Cycles 20, GB4003. http://dx.doi.org/10.1029/2005GB002672.

Durka, W., Schulze, E.-D., Gebauer, G., Voerkelius, S., 1994. Effects of forest decline on uptake and leaching of deposited nitrate determined from ^{15}N and ^{18}O measurements. Nature 372, 765–767.

Elliott, E.M., Kendall, C., Wankel, S.D., Burns, D.A., Boyer, E.W., Harlin, K., Bain, D.J., Butler, T.J., 2007. Nitrogen isotopes as indicators of NO_x source contributions to atmospheric nitrate deposition across the Midwestern and Northeastern United States. Environmental Science & Technology 41, 7661–7667.

Environment Canada, 2011. National Climate Data and Information Archive. http://www.climate.weatheroffice.gc.ca/climate_normals/results_e.html?stnID=2519&autofwd=1 (accessed May 2011).

Fang, Y.T., Koba, K., Wang, X.M., Wen, D.Z., Li, J., Takebayashi, Y., Liu, X.Y., Yoh, M., 2011. Anthropogenic imprints on nitrogen and oxygen isotopic composition of precipitation nitrate in a nitrogen-polluted city in southern China. Atmospheric Chemistry and Physics 11, 1313–1325.

Felix, J.D., Elliott, E.M., Shaw, S.L., 2012. Nitrogen isotopic composition of coal-fired power plant NO_x: influence of emission controls and implications for global emission inventories. Environmental Science & Technology 46, 3528–3535.

Fenn, M., Poth, M., 2004. Monitoring nitrogen deposition in throughfall using ion exchange resin columns: a field test in the San Bernardino Mountains. Journal of Environmental Quality 33, 2007–2014.

Fenn, M., Ross, C., 2010. Sulfur and nitrogen deposition in the Athabasca oil sands region. In: 103rd Annual Meeting of the Air & Waste Management Association, Extended Abstract 2010-A-664-AWMA, in Calgary, Canada.

Fenn, M.E., Poth, M.A., Aber, J.D., Baron, J.S., Bormann, B.T., Johnson, D.W., Lemly, A.D., McNulty, S.G., Ryan, D.F., Stottlemyer, R., 1998. Nitrogen excess in North American ecosystems: predisposing factors, ecosystem responses, and management strategies. Ecological Applications 8, 706–733.

Fenn, M.E., Jovan, S., Yuan, F., Geiser, L., Meixner, T., Gimeno, B.S., 2008. Empirical and simulated critical loads for nitrogen deposition in California mixed conifer forests. Environmental Pollution 155, 492–511.

Fenn, M.E., Allen, E.B., Weiss, S.B., Jovan, S., Geiser, L., Tonnesen, G.S., Johnson, R.F., Rao, L.E., Gimeno, B.S., Yuan, F., Meixner, T., Bytnerowicz, A., 2010. Nitrogen critical loads and management alternatives for N-impacted ecosystems in California. Journal of Environmental Management 91, 2404–2423.

Fenn, M.E., Sickman, J.O., Bytnerowicz, A., Clow, D.W., Molotch, N.P., Pleim, J.E., Tonnesen, G.S., Weathers, K.C., Padgett, P.E., Campbell, D.H., 2009. Methods for measuring atmospheric nitrogen deposition inputs in arid and montane ecosystems of western North America. In: Legge, A.H. (Ed.), Developments in Environmental Science, Air Quality and Ecological Impacts: Relating Sources to Effects, vol. 9. Elsevier, Amsterdam, pp. 179–228.

Fraser, M.P., Cass, G.R., 1998. Detection of excess ammonia emissions from in-use vehicles and the implications for fine particle control. Environmental Science & Technology 32, 1053–1057.

Freyer, H., 1991. Seasonal variation of $^{15}N/^{14}N$ ratios in atmospheric nitrate species. Tellus 43B, 30–44.

Galloway, J., Townsend, A., Erisman, J., Bekunda, M., Cai, Z., Freney, J., Martinelli, L., Seitzinger, S., Sutton, M., 2008. Transformation of the nitrogen cycle: recent trends, questions, and potential solutions. Science 320, 889–892.

Garten Jr., C.T., 1992. Nitrogen isotope composition of ammonium and nitrate in bulk precipitation and forest throughfall. International Journal of Environmental Analytical Chemistry 47, 33–45.

Government of Alberta, 2011. Agricultural and Rural Development, AgroClimatic Information Service. http://www.agric.gov.ab.ca/app116/quick.jsp (accessed April 2011).

Gruber, N., Galloway, J.N., 2008. An Earth-system perspective of the global nitrogen cycle. Nature 451, 293–296.

Hastings, M., Steig, E., Sigman, D., 2004. Seasonal variations in N and O isotopes of nitrate in snow at Summit, Greenland: implications for the study of nitrate in snow and ice cores. Journal of Geophysical Research 109, D20. http://dx.doi.org/10.1029/2004JD004991.

Hastings, M.G., Sigman, D., Lipschultz, F., 2003. Isotopic evidence for source changes of nitrate in rain at Bermuda. Journal of Geophysical Research 108, D24. http://dx.doi.org/10.1029/2003JD003789.

He, C.E., Wang, X., Liu, X.J., Fangmeier, A., Christie, P., Zhang, F.S., 2010. Nitrogen deposition and its contribution to nutrient inputs to intensively managed agricultural ecosystems. Ecological Applications 20, 80–90.

Heaton, T., 1986. Isotopic studies of nitrogen pollution in the hydrosphere and atmosphere: a review. Chemical Geology 59, 87–102.

Heaton, T., Spiro, B., Robertson, S., 1997. Potential canopy influences on the isotopic composition of nitrogen and sulphur in atmospheric deposition. Oecologia 109, 600–607.

Jung, K., Chang, S.X., 2012. Four years of simulated N and S depositions did not cause N saturation in a mixedwood boreal forest ecosystem in the oil sands region in northern Alberta, Canada. Forest Ecology and Management 280, 62–70.

Jung, K., Chang, S.X., Arshad, M.A.C., 2011. Effects of canopy-deposition interaction on H^+ supply to soils in *Pinus banksiana* and *Populus tremuloides* ecosystems in the Athabasca oil sands region in Alberta, Canada. Environmental Pollution 159, 1327–1333.

Kaiser, J., Hastings, M.G., Houlton, B.Z., Röckmann, T., Sigman, D.M., 2007. Triple oxygen isotope analysis of nitrate using the denitrifier method and thermal decomposition of N_2O. Analytical Chemistry 79, 599–607.

Kendall, C., 1998. Tracing nitrogen sources and cycling in catchments. In: Kendall, C., McDonnell, J. (Eds.), Isotope Tracers in Catchment Hydrology. Elsevier, pp. 519–576.

Kendall, C., Elliott, E., Wankel, S., 2007. Tracing anthropogenic inputs of nitrogen to ecosystems. In: Lajtha, K., Michener, R. (Eds.), Stable Isotopes in Ecology and Environmental Science. Blackwell Scientific Publications, pp. 375–449.

Larsen, C.P.S., 1997. Spatial and temporal variations in boreal forest fire frequency in northern Alberta. Journal of Biogeography 24, 663–673.

Lawrence, M.G., Crutzen, P.J., 1999. Influence of NO_x emissions from ships on tropospheric photochemistry and climate. Nature 402, 167–170.

Laxton, D.L., Watmough, S.A., Aherne, J., 2012. Nitrogen cycling in *Pinus banksiana* and *Populus tremuloides* stands in the Athabasca oil sands region, Alberta, Canada: Water. Air and Soil Pollution 223, 1–13.

Leahey, D.M., Hansen, M.C., 1982. Influences of terrain on plume level winds in the Athabasca oil sands area. Atmospheric Environment 16, 2849–2854.

Liu, X.J., Zhang, Y., Han, W.X., Tang, A.H., et al., 2013. Enhanced nitrogen deposition over China. Nature 494, 459–462.

Lü, C., Tian, H., 2007. Spatial and temporal patterns of nitrogen deposition in China: synthesis of observational data. Journal of Geophysical Research 112, D22S05. http://dx.doi.org/10.1029/2006JD007990.

Lyons, J., 2001. Transfer of mass-independent fractionation in ozone to other oxygen-containing radicals in the atmosphere. Geophysical Research Letters 28, 3231–3234.

MacDonald, J.A., Dise, N.B., Matzner, E., Armbruster, M., Gundersen, P., Forsius, M., 2002. Nitrogen input together with ecosystem nitrogen enrichment predict nitrate leaching from European forests. Global Change Biology 8, 1028–1033.

Michalski, G., Bhattacharya, S., 2009. The role of symmetry in the mass independent isotope effect in ozone. Proceedings of the National Academy of Sciences 106, 5493–5496.

Michalski, G., Böhlke, J.K., Thiemens, M., 2004. Long term atmospheric deposition as the source of nitrate and other salts in the Atacama Desert, Chile: new evidence from mass-independent oxygen isotopic compositions. Geochimica et Cosmochimica Acta 68, 4023–4038.

Michalski, G., Scott, Z., Kabiling, M., Thiemens, M., 2003. First measurements and modeling of $\Delta^{17}O$ in atmospheric nitrate. Geophysical Research Letters 30. http://dx.doi.org/10.1029/2003GL017015.

Moore, H., 1977. The isotopic composition of ammonia, nitrogen dioxide and nitrate in the atmosphere. Atmospheric Environment 11, 1239–1243.

Morin, S., Savarino, J., Frey, M.M., Yan, N., Bekki, S., Bottenheim, J.W., Martins, J.M.F., 2008. Tracing the origin and fate of NO_x in the Arctic atmosphere using stable isotopes in nitrate. Science 322, 730–732.

Nanus, L., Williams, M.W., Campbell, D.H., Elliott, E.M., Kendall, C., 2008. Evaluating regional patterns in nitrate sources to watersheds in national parks of the Rocky Mountains using nitrate isotopes. Environmental Science & Technology 42, 6487–6493.

NPRI, 2011. National Pollutant Release Inventory Online Data Search. Environment Canada. http://www.ec.gc.ca/pdb/websol/querysite/query_e.cfm (accessed November 2011).

Ok, Y., Chang, S.X., FENG, Y.S., 2007. Sensitivity to acidification of forest soils in two watersheds with contrasting hydrological regimes in the oil sands region of Alberta. Pedosphere 17, 747–757.

Pearson, J., Wells, D., Seller, K., Bennett, A., Soares, A., Woodall, J., Ingrouille, M., 2000. Traffic exposure increases natural ^{15}N and heavy metal concentrations in mosses. New Phytologist 147, 317–326.

Proemse, B.C., Mayer, B., 2012. Tracing industrial nitrogen and sulfur emissions in the Athabasca oil sands region using stable isotopes. In: Percy, K.E. (Ed.), Alberta Oil Sands: Energy, Industry and the Environment. Elsevier Science, Oxford, UK. http://dx.doi.org/10.1016/B978-0-08-097760-7.00011-1.

Proemse, B.C., Mayer, B., Chow, J.C., Watson, J.G., 2012a. Isotopic characterization of nitrate, ammonium and sulfate in stack $PM_{2.5}$ emissions in the Athabasca oil sands region, Alberta, Canada. Atmospheric Environment 60, 555–563.

Proemse, B.C., Mayer, B., Fenn, M.E., 2012b. Tracing industrial sulfur contributions to atmospheric sulfate deposition in the Athabasca oil sands region, Alberta, Canada. Applied Geochemistry 27, 2425–2434.

Sandhu, H., Blower, L., 1986. Acid-forming emissions in Alberta, Canada. Environmental Management 10, 689–695.

Savarino, J., Kaiser, J., Morin, S., Sigman, D.M., Thiemens, M.H., 2007. Nitrogen and oxygen isotopic constraints on the origin of atmospheric nitrate in coastal Antarctica. Atmospheric Chemistry and Physics 7, 1925–1945.

Schindler, D.W., Dillon, P.J., Schreier, H., 2006. A review of anthropogenic sources of nitrogen and their effects on Canadian aquatic ecosystems. Biogeochemistry 79, 25–44.

Sebilo, M., Mayer, B., Grably, M., Billiou, D., Mariotti, A., 2004. The use of the "ammonium diffusion" method for $\delta^{15}N-NH_4^+$ and $\delta^{15}N-NO_3^-$ measurements: comparison with other techniques. Environmental Chemistry 1, 99–103.

Seinfeld, J., Pandis, S., 2006. Atmospheric Chemistry and Physics, second ed.. In: From Air to Pollution to Climate Change John Wiley & Sons, Inc., pp. 1–1203

Sigman, D.M., Casciotti, K.L., Andreani, M., Barford, C., Galanter, M., Böhlke, J.K., 2001. A bacterial method for the nitrogen isotopic analysis of nitrate in seawater and freshwater. Analytical Chemistry 73, 4145–4153.

Simkin, S.M., Lewis, D.N., Weathers, K.C., Lovett, G.M., Schwarz, K., 2004. Determination of sulfate, nitrate, and chloride in throughfall using ion-exchange resins. Water, Air, and Soil Pollution 153, 343–354.

Simpson, D., Aas, W., Bartnicki, J., Berge, H., Bleeker, A., et al., 2011. Atmospheric transport and deposition of reactive nitrogen in Europe. In: Sutton, M.A., Howard, C.M., Erisman, J.W., Billen, G., Bleeker, A., Grennfelt, P., van Grinsven, H., Grizzetti, B. (Eds.), The European Nitrogen Assessment: Sources, Effects and Policy Perspectives. Cambridge University Press, New York, pp. 298–316.

Soil Classification Working Group, 1998. The Canadian System of Soil Classification, third ed. Agriculture and Agri-Food Canada Publication http://sis.agr.gc.ca/cansis/taxa/cssc3/intro.html. (accessed January 2012).

Thiemens, M., Heidenreich, J., 1983. The mass-independent fractionation of oxygen: a novel isotope effect and its possible cosmochemical implications. Science 219, 1073–1075.

Whitfield, C., Aherne, J., Watmough, S., 2009. Modeling soil acidification in the Athabasca oil sands region, Alberta, Canada. Environmental Science & Technology 43, 5844–5850.

Wieder, R., Vitt, D., Burke-Scoll, M., Scott, K., House, M., Vile, M., 2010. Nitrogen and sulphur deposition and the growth of *Sphagnum fuscum* in bogs of the Athabasca Oil Sands Region, Alberta. Journal of Limnology 69, 161–170.